Cell Death and Differentiation (2012) 19, 1709–1721

www.nature.com/cdd

AIM2/ASC triggers caspase-8-dependent apoptosis in *Francisella*-infected caspase-1-deficient macrophages

R Pierini[1,2], C Juruj[1,2], M Perret[1,2], CL Jones[3], P Mangeot[1,2], DS Weiss[3,4] and T Henry*[,1,2]

The inflammasome is a signalling platform leading to caspase-1 activation. Caspase-1 causes pyroptosis, a necrotic-like cell death. AIM2 is an inflammasome sensor for cytosolic DNA. The adaptor molecule ASC mediates AIM2-dependent caspase-1 activation. To date, no function besides caspase-1 activation has been ascribed to the AIM2/ASC complex. Here, by comparing the effect of gene inactivation at different levels of the inflammasome pathway, we uncovered a novel cell death pathway activated in an AIM2/ASC-dependent manner. *Francisella tularensis*, the agent of tularaemia, triggers AIM2/ASC-dependent caspase-3-mediated apoptosis in caspase-1-deficient macrophages. We further show that AIM2 engagement leads to ASC-dependent, caspase-1-independent activation of caspase-8 and caspase-9 and that caspase-1-independent death is reverted upon caspase-8 inhibition. Caspase-8 interacts with ASC and active caspase-8 specifically colocalizes with the AIM2/ASC speck thus identifying the AIM2/ASC complex as a novel caspase-8 activation platform. Furthermore, we demonstrate that caspase-1-independent apoptosis requires the activation of caspase-9 and of the intrinsic pathway in a typical type II cell manner. Finally, we identify the AIM2/ASC-dependent caspase-1-independent pathway as an innate immune mechanism able to restrict bacterial replication *in vitro* and control IFN-γ levels *in vivo* in Casp1^{KO} mice. This work underscores the crosstalk between inflammasome components and the apoptotic machinery and highlights the versatility of the pathway, which can switch from pyroptosis to apoptosis.

Cell Death and Differentiation (2012) **19,** 1709–1721; doi:10.1038/cdd.2012.51; published online 4 May 2012

The host cytosol has long been considered a safe haven for pathogens.[1] It is now clear that cytosolic bacteria are detected by innate immune pattern recognition receptors (PRRs). The inflammasome is an innate immune signalling platform sensing pathogens and danger signals leading to activation of the inflammatory caspase-1.[2,3] Active caspase-1 triggers the release of the inflammatory cytokines IL-1β and IL-18. Furthermore, caspase-1 triggers a necrotic-like cell death termed pyroptosis. Pyroptosis occurs within minutes after inflammasome activation and in contrast to apoptosis, is associated with immediate plasma membrane permeabilisation and release of cytoplasmic contents.[4,5] Caspase-1-dependent cell death is a key innate immune defence against intracellular bacteria by removing the pathogen's replication niche.[5,6]

Francisella tularensis is a highly infectious bacterium causing tularaemia in humans.[7] *F. tularensis* subspecies *novicida* (*F. novicida*) is considered non-pathogenic for humans and is widely used as a model to study highly virulent subspecies. In mice, *Francisella* is found mostly in myeloid cells such as macrophages and neutrophils.[8] Its ability to cause disease is tightly linked to its ability to rapidly escape from the phagosome into the host cytosol where it can replicate to very high numbers.[9,10] Deletion of a genetic locus, the *Francisella* Pathogenicity Island (FPI), abolishes the ability of *F. tularensis* to escape into the host cytosol.[11,12] The ΔFPI mutant remains in a vacuolar compartment, is unable to replicate intracellularly and is highly attenuated *in vivo*.

Infection with WT *F. novicida*, which escapes into the cytosol, triggers type I IFN secretion.[13,14] Furthermore, *Francisella* DNA released into the host cytosol upon bacteriolysis is detected by AIM2, an inflammasome receptor.[14–16] AIM2 activates caspase-1 via the inflammasome adaptor ASC.[17,18] Macrophages deficient for AIM2 (the receptor), ASC (the adaptor) or caspase-1 (the effector) do not trigger pyroptosis and do not release IL-1β upon *Francisella* infection or DNA transfection into the cytosol.[14–16] So far, there is no description of alternative pathways by which the AIM2/ASC complex could signal independently of the canonical inflammasome effector caspase-1.

Here, we tackled this issue using *F. novicida* infection, which is emerging as a key experimental model to study AIM2 inflammasome activation in a physiological manner. We carefully examined the kinetics and the cell death process in WT, AIM2-deficient (AIM2^{KO}), ASC^{KO} and Caspase-1-deficient (Casp1^{KO}) primary macrophages. We demonstrate that the AIM2/ASC complex acts as a novel caspase-8 activation

[1]Université de Lyon, Lyon, France; [2]INSERM U851, Lyon, France; [3]Emory Vaccine Center, Atlanta, GA, USA and [4]Division of Infectious Diseases, Emory University School of Medicine, Atlanta, GA, USA
*Corresponding author: T Henry, INSERM U851, Team 'Inflammasome and bacterial infections', Batiment Domilyon, Centre d'infectiologie, 321 avenue Jean Jaurés, Lyon 69007, France. Tel: +33 4 37 26 29 81; Fax: +33 4 37 28 23 41; E-mail: thomas.henry@inserm.fr
Keywords: inflammasome; bacterial infections; *Francisella*; AIM2; ASC; caspase-8
Abbreviations: BMM, bone marrow-derived macrophages; BMDC, bone marrow-derived dendritic cells; EtDi, ethidium homodimer; LDH, lactate dehydrogenase; *F. novicida*, *Francisella tularensis* subspecies *novicida*; FPI, *Francisella* pathogenicity island; PI, post-infection; MEEBO, mouse exonic evidence based oligonucleotide; PRR, pattern recognition receptors; TSB, tryptic soy broth; TUNEL, terminal deoxynucleotidyl transferase-mediated dUTP nick-end labelling
Received 1.8.11; revised 21.3.12; accepted 27.3.12; Edited by G Nunez; published online 04.5.12

platform and triggers apoptosis of infected Casp1^{KO} macrophages. Caspase-1-independent cell death was reversed by caspase-8 or -9 inhibition or by overexpression of Bcl-2 family members suggesting that the AIM2/ASC/caspase-8 complex triggers apoptosis by activating the mitochondrial apoptotic pathway. Importantly, we demonstrate that an ASC-dependent, caspase-1-independent pathway is a key to restrict intracellular *Francisella* replication *in vitro* and to control IFN-γ *in vivo*. The relevance of these pathways in caspase-1-proficient cells and animals remains to be investigated.

Results

AIM2 triggers ASC-dependent, caspase-1-independent cell death upon *Francisella* infection or DNA delivery into the cytosol. To investigate whether AIM2 or ASC could have additional functions besides activating caspase-1, we decided to carefully examine the phenotypes of murine macrophages deficient for inflammasome components at different levels of the pathway. Bone marrow-derived macrophages (BMM) were infected with *F. novicida* and monitored for cell death. As previously described[12] and as measured by lactate dehydrogenase (LDH) release (Figure 1a) or propidium iodide incorporation (Figure 1b), infection with *F. novicida* (strain U112) triggered WT macrophage death while infection with the vacuolar mutant (ΔFPI mutant) had no effect on cellular viability during the time frame of the experiment. Consistent with an observation by Mariathasan *et al.*,[12] we observed a hierarchical kinetic of cell death between WT, Casp1^{KO} and ASC^{KO} macrophages. Indeed, WT macrophages started to die at 6 h post-infection (PI), while LDH release was observed from Casp1^{KO} macrophages starting at 10 h PI. In contrast, death of ASC^{KO} macrophages was only observed at 24 h PI and when infected with a high MOI indicating that this cell death was associated with a very high intracellular bacterial burden. This differential cell death between Casp1^{KO} and ASC^{KO} macrophages was not because of a general resistance of ASC^{KO} macrophages to cell death as ASC^{KO} and Casp1^{KO} macrophages displayed similar susceptibility to gliotoxin-induced cell death (Figure 1c). We observed the same biphasic cell death upon *Francisella* infection of bone marrow-derived dendritic cells (BMDC) (Figure 1d). These results demonstrate that although in WT myeloid cells ASC activates caspase-1-mediated pyroptosis, in Casp1^{KO} cells ASC triggers an alternative cell death pathway.

We next investigated if activation of this novel ASC-dependent caspase-1-independent pathway was dependent on AIM2 or on NLRP3, another inflammasome receptor. As previously observed,[19] NLRP3^{KO} macrophages died with similar kinetics as WT macrophages (Figure 1e). In contrast, AIM2^{KO} macrophages phenocopied ASC^{KO} macrophages and were highly resistant to *F. novicida*-induced cell death. Consistent with the involvement of the IFN-inducible receptor AIM2,[14,15] prestimulation of Casp1^{KO} macrophages with IFN-β accelerated the cell death kinetic (Supplemental Figure S1). Pretreatment of ASC^{KO} macrophages with IFN-β did not render these cells susceptible to *F. novicida*-induced cell death.

To confirm the existence of an AIM2/ASC-dependent, caspase-1-independent cell death pathway, we assessed phosphatidylserine externalisation (annexin V labelling) and membrane permeabilisation (propidium iodide staining) by flow cytometry. *F. novicida*-infected WT macrophages died by pyroptosis and do not display apoptotic features.[20] Yet, a large propidium iodide^{neg} annexin V^{pos} population was observed in infected WT macrophages (Figure 1f). This suggested to us that annexin V staining could not be used to discriminate pyroptosis from apoptosis in primary macrophages. Nonetheless, annexin V staining kinetics perfectly correlated with LDH release kinetics. Indeed, as compared with uninfected macrophages, infected AIM2^{KO} and ASC^{KO} macrophages did not show any increase in annexin V labelling, whereas Casp1^{KO}, NLRP3^{KO} and WT macrophages displayed, respectively, a moderate-to-large increase in annexin V labelling. All together, these data highlighted a novel AIM2/ASC pathway triggering macrophage and dendritic cell death in the absence of caspase-1. As monitored by LDH release, Casp1^{KO} macrophages also died when transfected with p(dA/dT), whereas cytosolic DNA had no cytotoxic effect on ASC^{KO} macrophages (Figure 1g). As expected, this cell death in Casp1^{KO} BMM was delayed compared with caspase-1-mediated death occurring in WT macrophages. We conclude that this caspase-1-independent pathway is fully dependent on ASC. Importantly, this result demonstrates that the AIM2/ASC-dependent, caspase-1-independent cell death is not restricted to *F. novicida*-infected macrophages but is a general mechanism triggered upon AIM2 engagement.

The differential cell death between Casp1^{KO} and ASC^{KO} is not because of differences in bacterial entry, cytokine production, transcriptional responses or AIM2 activation kinetics. Cell death in WT and Casp1^{KO} BMM is dependent on the levels of intracellular *Francisella*, type I IFN and AIM2. One explanation for the differential cell death between ASC^{KO} and Casp1^{KO} could thus be because of a difference in one of these parameters. However, bacterial entry was similar in ASC^{KO} and Casp1^{KO} BMM (Supplemental Figure S2) and the increased cell death observed in Casp1^{KO} BMM was not associated with increased bacterial replication (see below). We did not detect any significant differences in TNF-α or type I IFN secretion between ASC^{KO} and Casp1^{KO} BMM following *F. novicida* infection (Supplemental Figure S3). Furthermore, we observed similar transcriptional responses to infection in ASC^{KO} and Casp1^{KO} macrophages (Figure 2a). Finally, we investigated AIM2 activation by following the intracellular dynamics of GFP-AIM2 (change from a diffuse cytosolic localisation to one spot within the cell to form a 'speck') (Figure 2b). We did not observe any difference in the kinetics of AIM2 speck formation (Figure 2c) between GFP-AIM2-expressing ASC^{KO} and Casp1^{KO} macrophages. We conclude that the differential cell death is due to specific AIM2/ASC signalling in Casp1^{KO} macrophages and not because of differences in bacterial entry/replication/lysis or in cytokine production between ASC^{KO} and Casp1^{KO} BMM. Furthermore, our data strongly suggest that the ASC-dependent caspase-1-independent pathway relies on post-transcriptional events.

Absence of caspase-1 switches AIM2/ASC-mediated death from pyroptosis to caspase-3-mediated apoptosis. In WT BMM, AIM2/ASC/caspase-1 triggers pyroptosis.

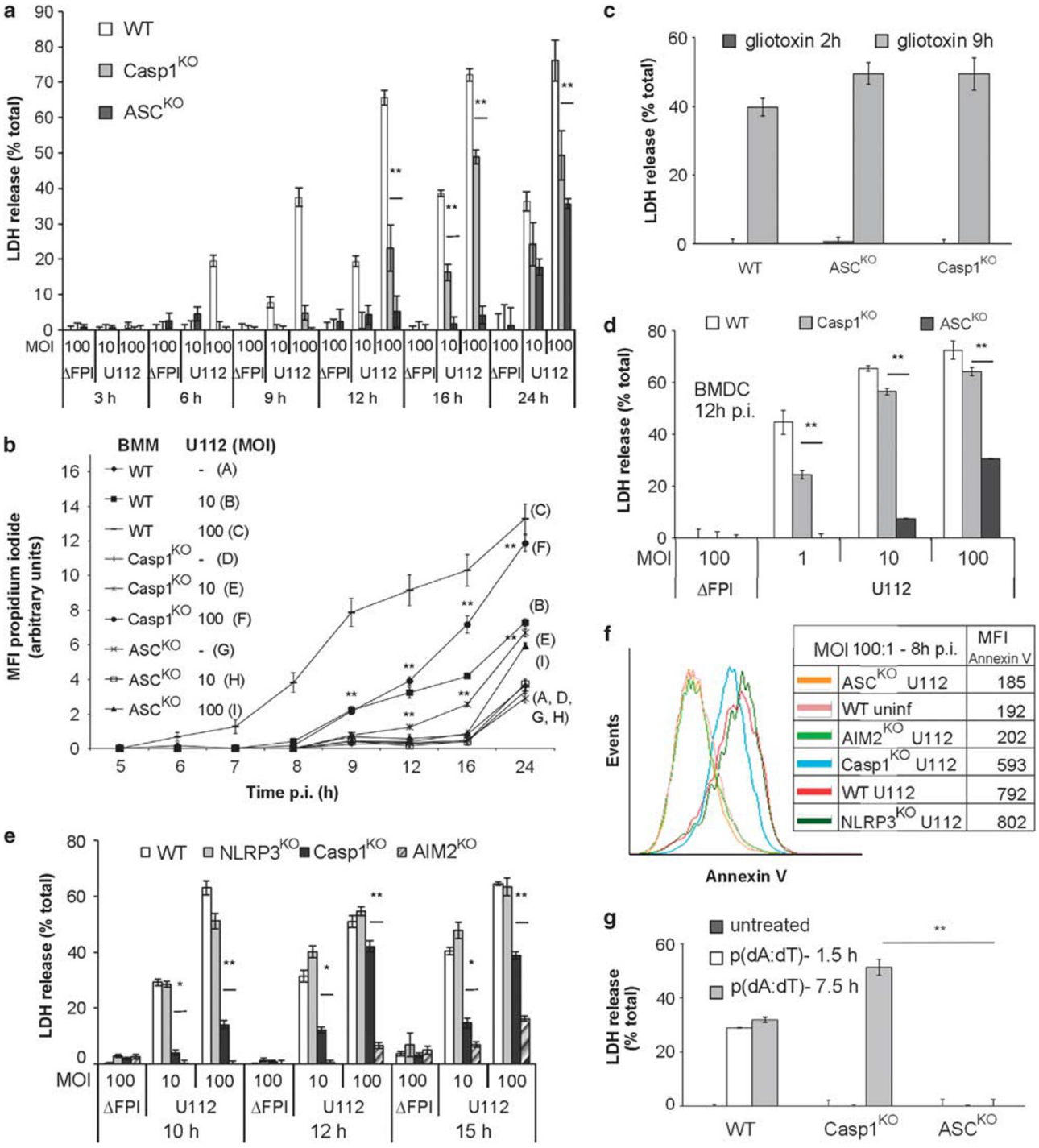

Figure 1 AIM2 triggers ASC-dependent, caspase-1-independent cell death upon *F. novicida* infection or DNA delivery into the cytosol. BMM death was assessed following U112 or ΔFPI mutant infection at the indicated MOI and time PI (**a, b, e** and **f**), following exposure to 5 μM gliotoxin (**c**), or following cell transfection with p(dA/dT) (**g**). (**a, c, d, e** and **g**) Cell death was determined by quantifying LDH levels in the culture medium. Results are expressed as percentage of total LDH release. Data are shown as mean ± S.E.M. ($n=5$). *$P<0.05$; **$P<0.01$. (**b**) Macrophages were incubated with propidium iodide (5 μg/ml). Cell death was determined by measuring propidium iodide fluorescence at the indicated time of PI, using a 96-well microplate fluorimeter. (**d**) BMDC death following infection with U112 or ΔFPI mutant for 12 h was assessed. (**f**) Cell death was determined by FITC-Annexin V/propidium iodide staining in BMM infected by U112 (MOI 100, 8 h PI). FITC fluorescence levels in propidium iodide-negative cells are shown, mean fluorescence intensity (MFI) is indicated. One experiment representative of three independent experiments is shown

Early membrane permeabilisation was visualised by the membrane impermeant dye ethidium homodimer (EtDi) (Figure 3a, top panel and Supplemental Movie SM1). This early membrane permeabilisation was concomitant with a rapid condensation and rounding up of the nucleus, in the absence of any obvious loss of cell adhesion properties.

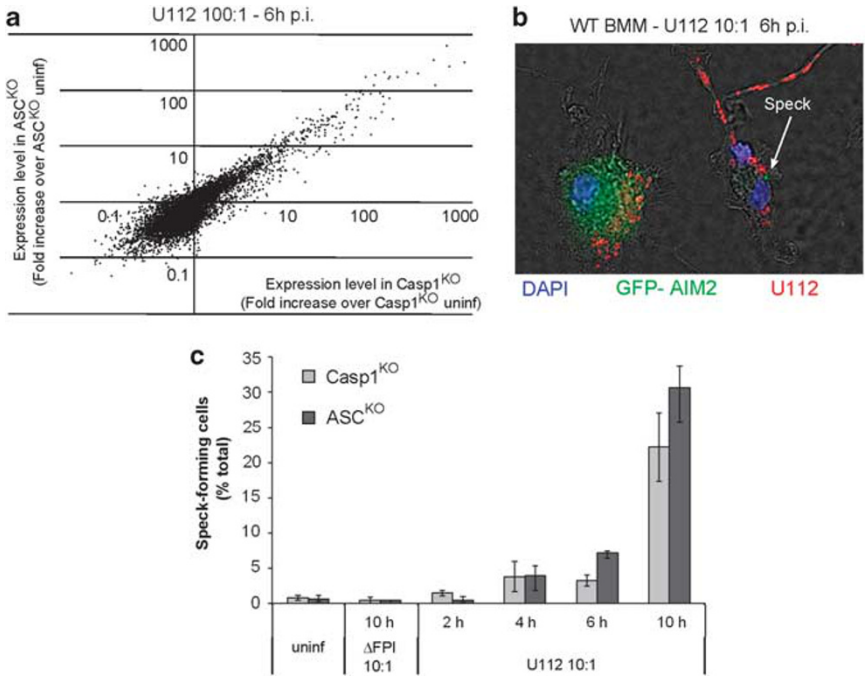

Figure 2 Differential cell death between Casp1^{KO} and ASC^{KO} BMM is not associated with differences in transcriptional responses or AIM2 activation. (**a**) Transcriptional changes as determined by microarray analysis in U112-infected Casp1^{KO} (plotted on the *x* axis) and ASC^{KO} BMM (plotted on the *y* axis) are shown. Each point represents expression level of single transcript at 6 h PI (MOI 100) normalised to its expression in the corresponding uninfected BMM. (**b**) Example of GFP-AIM2 speck formation in BMM following U112 infection. GFP-AIM2-expressing BMM (ASC^{KO} in the figure) were infected with U112 for 6 h (MOI 10). U112 bacteria were immunostained with a polyclonal anti-*F. novicida* antibody (red), and nuclei were labelled with DAPI. On the left, an infected BMM displayed diffuse cytosolic GFP-AIM2 pattern (no activation) while the cell on the right showed AIM2 activation as visualised by GFP-AIM2 relocalisation into a speck. (**c**) Speck-forming Casp1^{KO} and ASC^{KO} BMM following ΔFPI mutant or U112 infection were counted under the microscope. Results are expressed as mean ± S.E.M. ($n = 3$) and are representative of three independent experiments

None of these changes were observed upon infection with the ΔFPI mutant (Supplemental Movie SM2 and Supplemental Figure S4). In contrast, time-lapse video microscopy of *F. novicida*-infected Casp1^{KO} BMM revealed a very different course of events with a fast cellular contraction followed by a very delayed membrane permeabilisation (Figure 3a, bottom panel and Supplemental Movie SM3). The same genotype-dependent phenotypes were observed upon p(dA/dT) transfection (Figure 3b and Supplemental Movies SM4 and 5). In ASC-mCherry-expressing WT BMM, nuclear morphological changes were visible within minutes following inflammasome activation as visualised by ASC-mCherry speck formation (Figure 3b and Supplemental Movie SM4). Interestingly, in ASC-mCherry-expressing Casp1^{KO} macrophages, a marked delay was observed between speck formation and the first morphological change (cell shrinkage) (Figure 3b and Supplemental Movie SM5). This observation indicates that the two cell death mechanisms triggered downstream of ASC function very differently: one triggers cell death within minutes, whereas the other proceeds slowly to the cell death commitment point. The morphological changes observed in Casp1^{KO} BMM upon *Francisella* infection or p(dA/dT) transfection were evocative of an apoptotic death. It thus suggested that in the absence of caspase-1, AIM2/ASC-mediated cell death could switch from pyroptosis to apoptosis. Consistent with the latter mode of cell death, Casp1^{KO} macrophages infected with *F. novicida* showed condensed nuclei in the absence of membrane permeabilisation (EtDi negative nuclei) (Figures 3c–e), terminal deoxynucleotidyl transferase-mediated dUTP nick-end labeling positive (TUNEL^{+}) nuclei (Figure 3f, and Supplemental Figure S5), and characteristic DNA laddering (Figure 3g, left panel), three features not presented by WT or ASC^{KO} macrophages. In contrast, gliotoxin intoxication led to a typical DNA laddering pattern in WT, Casp1^{KO} and ASC^{KO} macrophages (Figure 3g, right panel).

Apoptosis is defined by morphological criteria and in most cases by caspase-3 activation. We used Ac-DEVD-AMC, a fluorogenic substrate, to monitor caspase-3/7 activities. At 8, 10 and 11 h PI (Figure 4a and data not shown), Casp1^{KO} macrophages displayed a high DEVDase activity, which was dependent on infection with WT *F. novicida* and on the MOI (Figure 4a). DEVDase activity was not observed in WT or ASC^{KO} macrophages at any of the time points tested. We did not observe caspase-7 activation by western blot in Casp1^{KO} macrophages (data not shown). However, we detected caspase-3 activation as early as 6 h PI in *F. novicida*-infected Casp1^{KO} BMM, but not in WT or ASC^{KO} BMM (Figure 4b). In agreement with caspase-3-dependent apoptosis, we detected a significant reduction in Casp1^{KO} macrophage death upon DEVD-fluoromethyl ketone (FMK) addition (25 to 33% reduction) (Figure 4c). In contrast, DEVD-FMK treatment did not reduce *F. novicida*-mediated cell death in WT macrophages (Supplemental Figure S6).

Caspase-8 triggers AIM2/ASC-dependent apoptosis. Casp1^{KO} macrophages do not express caspase-11, the

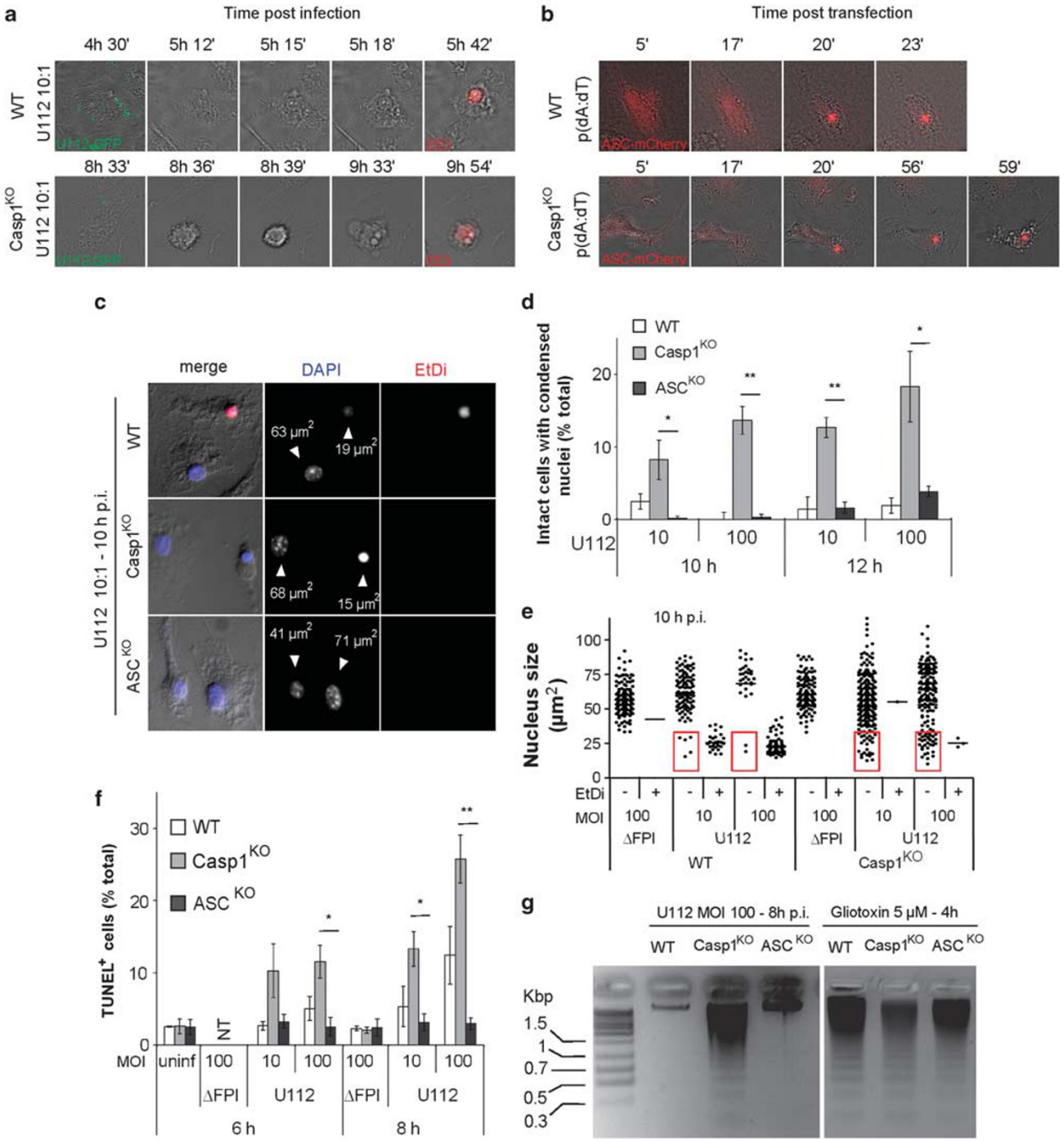

Figure 3 *F. novicida*-infected Casp1^{KO} BMM die in an apoptotic manner. (**a**) Analysis of changes in cell morphology and cell membrane permeabilisation were investigated by time-lapse video microscopy in WT and Casp1^{KO} BMM, infected with U112 (MOI 10). Loss of integrity of the plasma membrane was visualised by EtDi fluorescence. Infection by GFP-expressing U112 was checked at the first time point thanks to GFP signal. (**b**) Detection of inflammasome speck formation and observation of changes in cell morphology in WT and Casp1^{KO} BMM following transfection with p(dA/dT) were performed by time-lapse investigation of ASC-mCherry-transduced macrophages. Apparent large size of ASC-mCherry speck is owing to the overexposure required to visualise the weaker ASC-mCherry diffuse signal. (**c**) Delay between cell shrinkage, nuclear condensation and cell membrane permeabilisation was observed in Casp1^{KO} BMM, but not in WT and ASC^{KO} BMM. Condensed nuclei had a reduced size and non-detectable nucleoles by DAPI staining. Cell permeabilisation was observed by EtDi staining. (**d**) Cells with condensed nuclei and intact cell membrane (no EtDi staining) were quantified by microscopy. Results are expressed as mean ± S.E.M. ($n=3$), and are representative of three independent experiments. *$P<0.05$; **$P<0.01$. (**e**) Nucleus size was determined at 10 h PI using Image J software. Nuclei were classified as either EtDi positive (EtDi^{+}) or negative (EtDi^{-}). EtDi^{-}, condensed nuclei, which are highlighted in the red squares were more prevalent in Casp1^{KO} than in WT BMM. (**f**) TUNEL assay was performed on macrophages infected with the indicated strains at the indicated MOI and at the indicated time of PI. The percentage of cells containing TUNEL^{+} nuclei was quantified by microscopy. Results are expressed as mean ± S.E.M. ($n=3$), and are representative of three independent experiments. *$P<0.05$; **$P<0.01$. (**g**) Ladder-like DNA fragmentation was observed in Casp1^{KO} BMM, but not in WT and ASC^{KO}, infected with U112 (MOI 100) for 8 h. Conversely, DNA laddering was observed in WT, Casp1^{KO} and ASC^{KO} macrophages after a 5-h treatment with 5 μM gliotoxin. Fragmented soluble DNA from 10^6 BMM was loaded in each lane. Results are from one experiment representative of three independent experiments. NT, not tested

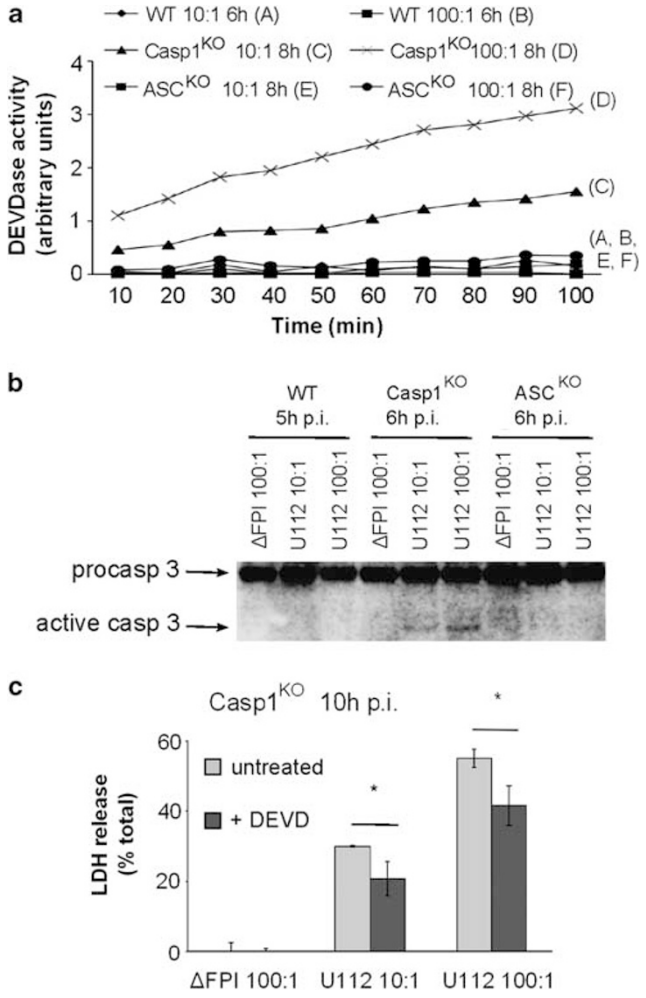

Figure 4 Apoptosis in Casp1^{KO} BMM following *F. novicida* infection is mediated by caspase-3. (**a**) Caspase-3/7 activity was investigated by measuring fluorescence signal emitted upon Ac-DEVD-AMC hydrolysis when incubated with protein lysates from U112-infected WT (6 h PI), Casp1^{KO} and ASC^{KO} BMM (8 h PI). (**b**) Caspase-3 processing was monitored by western blot analysis in WT BMM infected with U112 or ΔFPI mutant for 5 h, and Casp1^{KO} and ASC^{KO} BMM infected for 6 h. (**c**) Effect of caspase-3 inhibitor Z-DEVD-FMK in reverting Casp1^{KO} BMM death following infection with U112 for 10 h. Results are expressed as percentage of total LDH release. Data are shown as mean ± S.E.M. ($n = 3$), *$P < 0.05$. Results are representative of three independent experiments

homologue of human caspase-4/5.[21,22] BMM express a low level of caspase-12.[23] We thus ruled out a role for these inflammatory caspases in AIM2/ASC-dependent apoptosis. In mice, initiator caspases include caspase-2, -8 and -9. We analysed activation of these caspases to determine if caspase-3-mediated apoptosis was associated with activation of apical caspases. We performed this analysis at early time points in order to focus only on the primary caspase activation events. We detected caspase-8 and caspase-9 processing in Casp1^{KO} macrophages infected with WT *F. novicida* at 8 h PI. (Figures 5a and b). The increase in the cleaved forms of caspase-8 and -9 was abolished upon infection with the ΔFPI mutant suggesting that caspase activation was resulting from detection of cytosolic bacteria. Accordingly, we did not observe any increase in caspase-8 or caspase-9 processing upon infection in ASC^{KO} and AIM2^{KO} BMM. These data indicate that in Casp1^{KO} macrophages, the AIM2/ASC complex triggers caspase-8 and -9 processing. To investigate the role of caspase-2 in caspase-1-independent cell death, we generated double knock-out animals for caspase-1 and caspase-2. *F. novicida* infection triggered cell death in Casp1Casp2^{DKO} with the same kinetics as in Casp1^{KO}, indicating that caspase-2 is not involved in ASC-dependent caspase-1-independent cell death (Supplemental Figure S7). Consistent with this result and although we observed a decrease in procaspase-2 levels at 7 and 8 h PI in WT and Casp1^{KO} BMM, respectively, (Figure 5b) we failed to detect any caspase-2 processed form at any time point despite the use of three different anti-caspase-2 antibodies (data not shown).

To functionally test the role of caspase-8 and -9, we first tried to knock-down their expression. However, in primary macrophages, using shRNA or siRNA techniques, we failed to obtain knock-down level higher than 30 to 60% at the protein level for these two targets without affecting cell viability (data not shown). On the basis of similar experiments performed on modulating caspase-1 expression levels, we believe such an efficacy of knock-down is too low to affect cell death kinetics (data not shown and Supplemental Figure S8). We thus tested caspase inhibitors for their ability to inhibit caspase-1-independent cell death. The caspase-8 inhibitor (IETD-FMK, 50 μM) significantly reduced caspase-1-independent cell death (51 to 68% reduction), whereas the caspase-2 inhibitor had no effect (Figure 5d). The caspase-9 inhibitor (LEHD-chloromethyl ketone (CMK)) had no effect at 50 μM. Knowing the higher specificity conferred by the less-reactive FMK group as compared with the CMK group, we also tested the LEHD-CMK inhibitor at 200 μM. At this latter concentration, the inhibitor was effective at inhibiting caspase-1-independent cell death (51 to 77% reduction). These results demonstrate that caspase-8 and possibly caspase-9 are instrumental in triggering AIM2/ASC-dependent, caspase-1-independent cell death. In contrast, caspase-2, a caspase involved in *Salmonella*-induced Casp1^{KO} macrophage cell death,[24] does not have a role in AIM2/ASC-dependent caspase-1-independent cell death.

The AIM2/ASC complex is a caspase-8 activation platform in Casp1^{KO} macrophages. Caspase-1 activation occurs through interaction of its CARD domain with the CARD domain of ASC. Active caspase-1 cleaves pro-IL-1β leading to IL-1β secretion. Caspase-1 activation can thus be monitored in a sensitive way by quantifying the IL-1β concentration in the cell supernatant. We took advantage of this property to screen ASC for functional interaction with other initiator caspase prodomains. As presented in Figure 6a, we generated chimeric caspases containing the CARD (caspase-2, -9, -11, -12) or the DED domain (caspase-8) of apical caspases fused to the active domain of caspase-1. We then used an inflammasome-reconstitution system in which 293T cells transiently expressed pro-IL-1β, AIM2 and either of the chimeric caspases in the presence or absence of ASC. As expected, procaspase-1 led to a large increase in IL-1β release upon ASC addition (Figure 6b). Interestingly, the chimeric DED$_{casp8}$-Casp1 triggered a large, ASC-dependent, IL-1β release indicating a functional

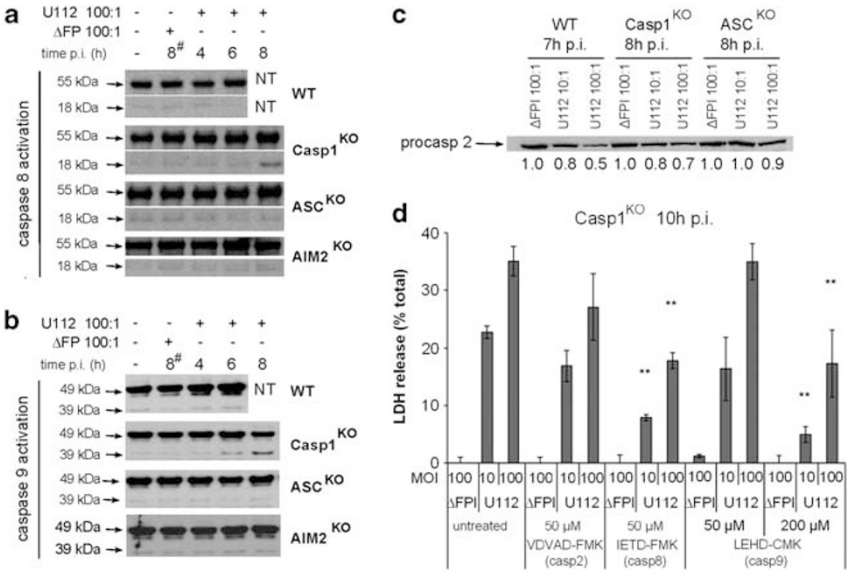

Figure 5 Caspase-8 and -9 are processed in *F. novicida*-infected Casp1^{KO} macrophages and their inhibition reverts caspase-1-independent cell death. Caspase-8 (**a**) and -9 (**b**) cleavage were investigated by immunoblot analysis in WT, Casp1^{KO} and ASC^{KO} BMM infected with U112 (MOI 100 : 1) at the indicated time post-infection or ΔFPI mutant (MOI 100 : 1) at 8 h PI. The 8 h PI time point was not investigated in WT macrophages due to high cell death level. '8$^{\#}$': ΔFPI mutant (MOI 100 : 1) -infected WT BMM were analysed at 6 h PI. (**c**) Decrease in procaspase-2 levels was assessed in U112- or ΔFPI mutant-infected WT BMM at 7 h PI, and Casp1^{KO} and ASC^{KO} BMM at 8 h PI. Procaspase-2 quantification normalised to ΔFPI-infected control is shown. (**d**) Cell death levels were determined by LDH assay in *F. novicida*-infected Casp1^{KO} BMM upon treatment with caspase-2 (Z-VDVAD-FMK), caspase-8 (Z-IETD-FMK) and caspase-9 (Ac-LEHD-CMK) inhibitors. Data are shown as mean ± S.E.M. ($n=3$). $^{*}P<0.01$. One experiment representative of three independent experiments is shown. NT, not tested

interaction between the DED domains of caspase-8 and ASC. In contrast, none of the other CARD domains (caspase-2, -9, -11 and -12) displayed any ASC-dependent function in this assay. This result suggests that ASC activates caspase-8 by a direct interaction with its DED domain.

We then assessed whether ASC interacts with caspase-8 in primary macrophages by co-immunoprecipitation experiments. Caspase-8 immunoprecipitated with ASC in uninfected Casp1^{KO} macrophages suggesting some level of constitutive interaction between ASC and pro-caspase-8 (Figure 6c). At 6 h PI, the level of caspase-8 protein immunoprecipitated with ASC was greatly enhanced indicating that caspase-8 interaction with ASC is increased upon *F. novicida* infection. This increased association between ASC and caspase-8 was maintained at 8 h PI in the presence of the caspase-8 inhibitor (z-IETD-FMK). In absence of caspase-8 inhibitor, the level of caspase-8 protein immunoprecipitated with ASC at 8 h PI went back to the level observed in uninfected macrophages likely due to the cleavage/activation of ASC-associated caspase-8 (Figure 5a). Overall, these two experiments suggest that caspase-8 interacts with ASC leading to its processing and activation.

As described above, sensing of *F. novicida* in the cytosol is associated with the formation of a large protein complex consisting of polymerised AIM2 and ASC, which can be visualised as a speck by immunofluorescence microscopy.[14] As AIM2/ASC specks are caspase-1 activation platforms, we wondered if they could also have such a role for caspase-8. We thus used fluorescently labelled caspase-8 (Carboxyfluorescein-LEDT-FMK) or caspase-9 (Carboxyfluorescein-LEHT-FMK) inhibitors to probe the localisation of active caspases in Casp1^{KO} macrophages. Strikingly, the active caspase-8 probe overlapped with the AIM2 and ASC specks in infected Casp1^{KO} macrophages (Figure 6d). Furthermore, the active caspase-9 probe was not visualised in the AIM2 or ASC specks in Casp1^{KO} macrophages (Figure 6d). In WT infected macrophages, we observed the presence of both caspase-8 and caspase-9 probes tightly associated with ASC specks (data not shown). However, this staining was likely due to non-specific binding of the probe to active caspase-1. To exclude any bias associated with the specificity of the probes, we investigated the localisation of the caspases directly by immunofluorescence. In the absence of antibodies suitable for detection of endogenous caspases by microscopy, we ectopically expressed FLAG-tagged caspase-8 or caspase-9 prodomains in WT and Casp1^{KO} macrophages. We detected the caspase-8 prodomain in more than 75% of the ASC specks formed in both WT and Casp1^{KO} macrophages (Figure 6e). In contrast, we could not detect colocalization of ASC with ectopically expressed FLAG peptide (<3%) or with the prodomain of caspase-9 (0%) (Figure 6e and Supplemental Figure S10A). Furthermore, neither FLAG-tagged caspase-8 prodomain (Supplemental Figure S10B) nor active caspase-8 probe (Supplemental Figure S9) colocalized with the AIM2 speck in ASC^{KO} macrophages indicating that ASC is an adaptor required for caspase-8 recruitment to the AIM2 speck. Taken together, these results clearly demonstrate that the AIM2/ASC complex acts as a novel platform capable of directly recruiting and activating caspase-8.

We could not detect direct caspase-9 activation in the AIM2/ASC complex suggesting that caspase-9 might be activated through caspase-8 cleavage of Bid and subsequent

activation of the mitochondrial intrinsic apoptotic pathway. In agreement with such an involvement, overexpression of Bcl-2 (Figure 6f) or Bcl-X_L (Supplemental Figure S11) reverted cell death in Casp1^{KO} but not in WT BMM (Supplemental Figures S12 and S13). We thus propose that Casp1^{KO} macrophages behave as type II cells and that full-blown caspase-3-dependent apoptosis mediated by AIM2/ASC-dependent caspase-8 activation requires cross-activation of the mitochondrial intrinsic pathway of apoptosis and of caspase-9 (Figure 6g).

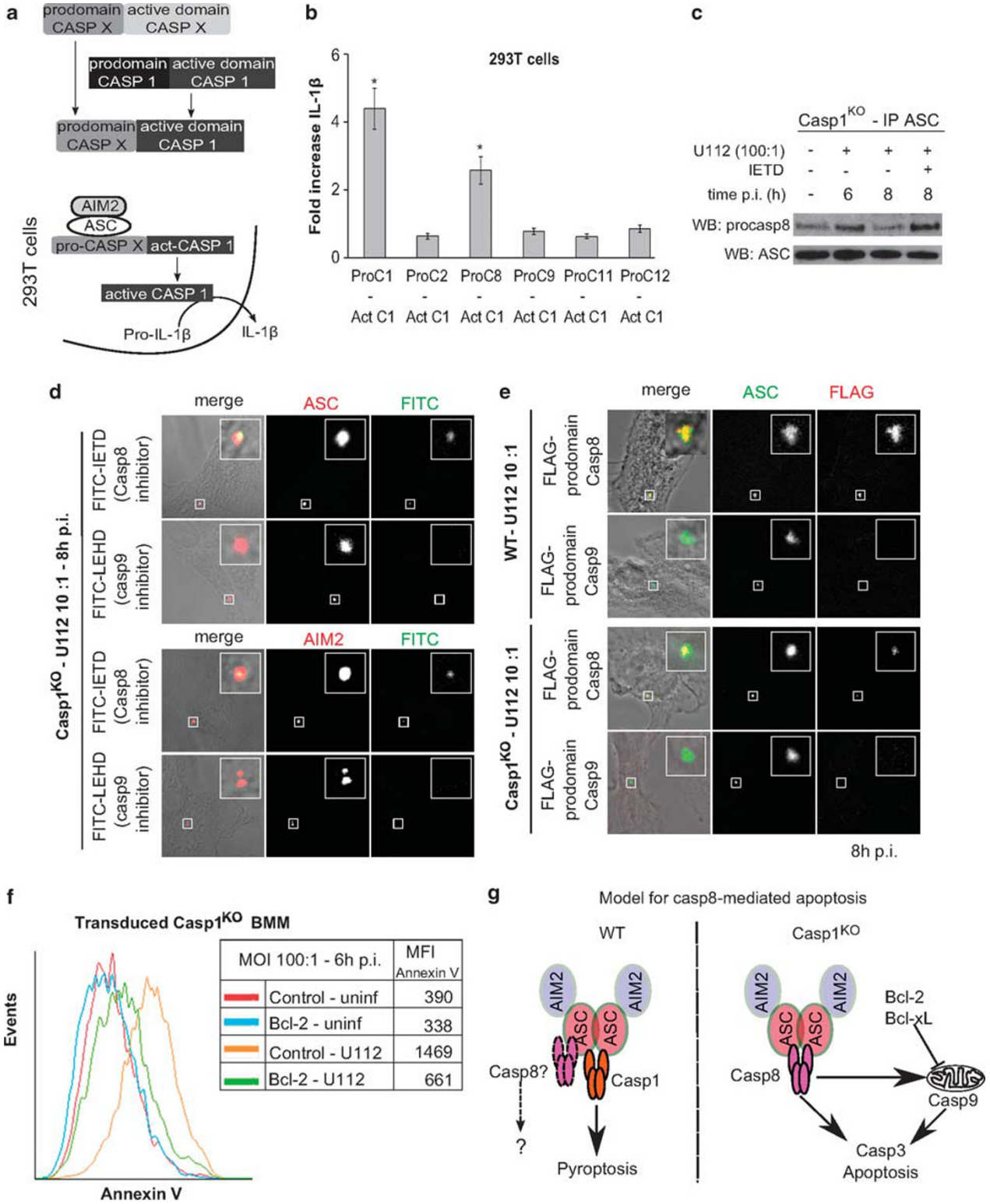

The ASC-dependent caspase-1-independent pathway restricts *F. novicida* intracellular replication and controls IFN-γ levels *in vivo* in Casp1^{KO} mice. As the AIM2/ASC/caspase-1 pathway is a key to restrict intracellular *F. novicida* growth, we wondered if the novel AIM2/ASC/caspase-8 pathway was also effective in limiting intracellular replication in Casp1^{KO} macrophages. Indeed, at 12 h PI, we observed a drastic increase in intracellular bacterial levels in ASC^{KO} macrophages as compared with Casp1^{KO} BMM (Figure 7a). This replication assay was further confirmed by flow cytometry analysis of BMM infected with GFP-expressing *F. novicida* (Figure 7b). These results imply that ASC-dependent caspase-1-independent death is a key to limiting intracellular bacterial replication in Casp1^{KO} macrophages and define this novel pathway as an antibacterial innate immune pathway. To investigate the importance of this pathway *in vivo*, we infected ASC^{KO} and Casp1^{KO} mice with *F. novicida.* We did not observe any significant differences in survival or bacterial burdens at 48 h PI in ASC^{KO} compared with Casp1^{KO} mice (Figure 8a and data not shown). However, at this same time point, the levels of IFN-γ, a key cytokine to fight intracellular bacteria were significantly higher in the serum of Casp1^{KO} animals as compared with ASC^{KO} animals (Figure 8b). In addition, the level of IFN-γ was higher in WT animals as compared with Casp1^{KO} animals. The differences observed in cell death *in vitro* (WT > Casp1^{KO} > ASC^{KO}) are thus perfectly mirrored by the differences observed *in vivo* in terms of IFN-γ. The role of caspase-8 in the ASC-dependent, caspase-1-independent production of IFN-γ remains to be investigated.

Discussion

AIM2 has recently been identified as a cytosolic DNA sensor capable of activating caspase-1 in an ASC-dependent manner.[17,18,25,26] Accordingly, in WT macrophages, AIM2 engagement leads to ASC-dependent, caspase-1-mediated pyroptosis. By comparing macrophages deficient at various levels of the inflammasome pathway, we uncovered a novel activity for the AIM2/ASC complex that is independent of the canonical inflammasome effector caspase-1. Our results demonstrate that upon cytosolic DNA sensing, Casp1^{KO} macrophages die via caspase-3-dependent apoptosis. We identified caspase-8 as the initiator caspase triggering this apoptosis. We showed that active caspase-8 is present in the AIM2/ASC complex in Casp1^{KO} macrophages and possibly in WT macrophages. Finally, we have demonstrated biochemically and functionally that ASC interacts with caspase-8. Taken together, our results identify the AIM2/ASC complex as a novel caspase-8 activation platform. Importantly, all of this work was performed in primary cells with a physiological stimulus. It confirms previous work done in human immortalised cell lines showing an interaction of ASC with caspase-8.[27-31] hASC interacts with BAX leading to

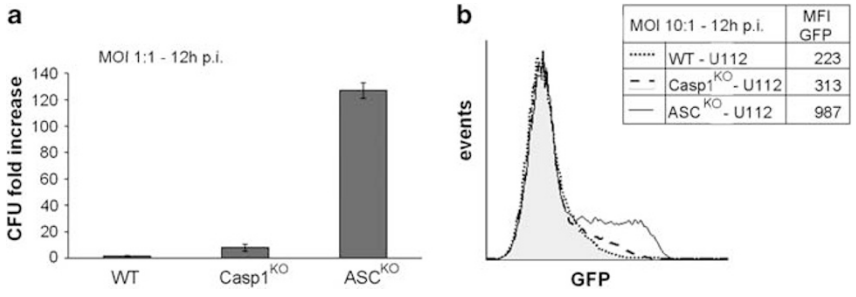

Figure 7 The ASC-dependent apoptosis restricts intracellular *F. novicida* replication in Casp1^{KO} macrophages *in vitro.* (**a**) Analysis of intracellular bacterial population in WT, Casp1^{KO} and ASC^{KO} BMM, after cell infection with U112 (MOI 1) for 12 h. Results are shown as mean ± S.E.M. ($n = 3$) and are representative of three independent experiments. (**b**) Bacterial replication was assessed by measuring GFP-fluorescence levels emitted by intracellular GFP-expressing U112 (MOI 10) at 12 h PI in WT, Casp1^{KO} and ASC^{KO} BMM

Figure 6 Caspase-8 functionally interacts with ASC within the AIM2/ASC speck. (**a**) Diagram of inflammasome-like pathway reconstitution in 293T cells. (**b**) The different initiator caspase prodomains (CARD domains for caspase-1, -2, -9, -11, -12 and DED domain for caspase-8) were fused to the active domain of caspase-1 and screened for functional interaction with the AIM2/ASC complex. Inflammasome-like pathway was reconstituted by cotransfecting 293T cells with plasmids expressing AIM2, ASC, pro-IL-1β and either of the chimeric caspases. Interaction of ASC with CARD$_{casp1}$ and DED$_{casp8}$ chimeric proteins led to IL-1β release. Analysis of IL-1β concentration in culture medium of 293T was determined by ELISA. Results are presented as IL-1β concentration fold increase between 293T cotransfected with AIM2, ASC, pro-IL-1β and either of the chimeric proteins versus cells undergoing the same cotransfection except for the absence of ASC-encoding plasmid. Raw values were typically 50 pg/ml of IL-1β in the absence of ASC and reached 250 pg/ml upon ASC addition. Data are shown as mean ± S.E.M. ($n = 9$). *$P < 0.05$. One experiment representative of three independent experiments is shown. (**c**) Casp1^{KO} macrophages were infected with U112 (MOI 100 : 1) for the indicated times. When indicated, the caspase-8 inhibitor (z-IETD-FMK at 50 μM) was added at 1 h PI. Endogenous ASC protein was immunoprecipitated from 10^7 cells. The level of ASC and caspase-8 (co)immunoprecipitated were analysed by immunoblot. One experiment out of two independent experiments is shown. (**d**) Casp1^{KO} macrophages were infected for 8 h with U112 at a MOI of 10 : 1. Endogenous ASC (top panel) and AIM2 (lower panel) proteins were detected by immunofluorescence. Active caspase-8 and caspase-9 were detected by a FITC-IETD and a FITC-LEHD probes, respectively. (**d** and **e**) Image dimensions are as follows: 30 × 30 μm^2. The insets (3 × 3 μm^2) correspond to 10-fold magnification of the ASC or Aim2 specks. (**e**) WT (top panel) and Casp1^{KO} (bottom panel) macrophages were transduced with lentiviruses encoding FLAG-Casp8-DED domain or FLAG-Casp9-CARD domain. 96 h post-transduction, macrophages were infected with U112 at a MOI of 10 : 1 for 8 h. Endogenous ASC protein and ectopically expressed FLAG-tagged-fusion proteins were detected by immunofluorescence. (**f**) Casp1^{KO} macrophages were transduced with Bcl-2-encoding or control lentiviruses. 96 h post-transduction, macrophages were infected with U112 at a MOI of 100 : 1 for 6 h. Cell death was determined by flow cytometry following annexin V-APC staining. Doublets and cell debris were excluded from the analysis based on FSC-H, FSC-A and SSC-A parameters. (**g**) Model for AIM2/ASC cell death pathways in WT and Casp1^{KO} macrophages (see text for details)

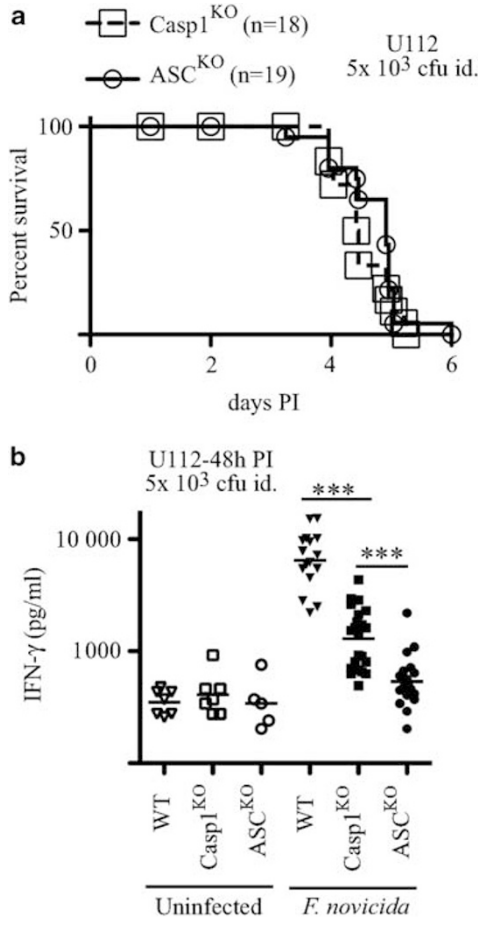

Figure 8 An ASC-dependent pathway controls IFN-γ levels during tularaemia in Casp1^{KO} mice. (**a**) Casp1^{KO} mice ($n=18$, dashed line, square symbols) and ASC^{KO} mice ($n=19$, plain line, round symbols) were infected with 5×10^3 *F. novicida* strain U112 CFU intradermally. Survival was monitored twice a day for 6 days. (**b**) WT, Casp1^{KO} and ASC^{KO} mice were infected with 5×10^3 U112 CFU. IFN-γ levels in serum were determined at 48 h PI by multiplex immunoassay. Each point represents the value obtained for one mouse. Geometric mean is shown. Mann–Whitney statistical analysis was performed. Two-tailed *P*-value is shown

caspase-9 activation.[31] We do not know if such a pathway is active in primary murine macrophages. Bcl-2 or Bcl-X_L overexpression inhibits ASC-dependent caspase-1-independent cell death (Figure 6f). Based on the direct activation of caspase-8 in the AIM2/ASC speck, we favour the hypothesis that caspase-9 activation is an event downstream of caspase-8 activation,[32] that macrophages are type II cells, that caspase-8 activation requires a mitochondrial relay to activate caspase-9 and trigger caspase-3-dependent apoptosis (see our model in Figure 6g).

Several innate immune pathways are known to activate initiator caspases during infections. For example, TLR2 engagement leads to caspase-8 activation.[33] We did not observe significant and reproducible caspase-8 activation in WT macrophages using western blotting analysis. We were thus unable to assess the role of TLR2 for caspase-8 activation (Supplemental Figure S14). Furthermore, we did not observe any differences in cytokine levels or in the kinetics of IκBα degradation (Supplemental Figure S15) between Casp1^{KO} and ASC^{KO} macrophages, suggesting that the ASC-dependent caspase-1-independent cell death is not because of differential levels of cytokine production or NF-κB activation.

Our work has uncovered the novel AIM2/ASC-dependent apoptotic pathway because of the use of macrophages deficient for caspase-1. Such a strategy has been widely used in the past and has revealed novel physiological cell death pathways occurring in the wild-type context such as necroptosis.[34] *In vitro*, in *Francisella*-infected WT macrophages, inflammasome activation triggers a fast caspase-1-mediated cell death, and thus the ASC-dependent caspase-1-independent pathway might not have time to impact cell function. Indeed, using macrophages from caspase-8 RIP3 double knock-out mice,[35] we did not detect any role for caspase-8 in caspase-1-mediated death (Supplemental Figure S16). However, such an innate immune pathway might be important in WT cells during sublethal inflammasome activation.[36] An ASC/caspase-8-dependent pathway has been described in immortalised cell lines[37] not expressing caspase-1.[38] We have detected both ASC and caspase-1 in CD4 and CD8 T cells as well as in B cells (data not shown) indicating that caspase-1 expression is not restricted to myeloid cells. At this time, we do not know if such cells exist in a physiological context. Finally, caspase-8 has numerous functions independent of leading to cell death. The role of the AIM2/ASC complex in modulating the caspase-8 non-lytic functions remains to be investigated.

Caspase-1-mediated pyroptosis is a key immune defence against intracellular bacteria by removing their replication niche.[6] We show here that in the absence of caspase-1, activation of the innate immune receptor AIM2 is still able, in an ASC-dependent manner, to restrict *Francisella* intracellular replication (Figures 7a and b). We did not observe any significant differences in survival or bacterial burden at 48 h PI between Casp1^{KO} and ASC^{KO} animals during experimental tularaemia (Figure 8a and data not shown). However, at 48 h PI, we detected a strong and specific reduction in the level of IFN-γ in ASC^{KO} as compared with Casp1^{KO} animals (Figure 8b and data not shown). This result indicates the presence of an ASC-dependent pathway occurring *in vivo* in Casp1^{KO} animals and regulating IFN-γ serum levels. Futures studies are needed to test whether this ASC-dependent caspase-1-independent pathway relies on caspase-8 and whether it regulates IFN-γ levels in caspase-1-proficient animals. While our manuscript was under revision, Gringhuis *et al*.[39] found that Dectin-1, in response to extracellular pathogens, can trigger caspase-8-mediated pro-IL-1β cleavage in an ASC-dependent, caspase-1-independent manner indicating the relevance of such a non-canonical inflammasome pathway in WT animals. Importantly, we demonstrate here that in absence of caspase-1, sensing of intracytosolic pathogen via AIM2 can also trigger ASC-mediated caspase-8 activation and apoptotic cell death.

Interestingly, another inflammasome sensor, NLRP1 (formerly known as Nalp1) interacts with components of the apoptotic pathway, Bcl-2, Bcl-X_L and Apaf1.[40] Here, we demonstrate that the AIM2/ASC complex can activate caspase-8. Taken together, these results highlight the interplay between the inflammasome pathway and the apoptotic machinery and illustrate the possible switch between apoptotic and pyroptotic pathways upon PRR engagement.

Materials and Methods

Mice and *in vivo* infections. This study was carried out in strict accordance with the French recommendations in the guide for the ethical evaluation of experiments using laboratory animals (http://circor.net/qui/ethicalEvaluationGuide4LaboratoryAnimals.pdf) and the European guidelines 86/609/CEE. All experimental studies were approved by the bioethic committee CECCAPP (protocols #ENS_2009_020 and #ENS_2011_006). Mice were in the C57BL/6 background. WT mice were purchased from Charles River Laboratories (Wilmington, MA, USA). ASC^{KO} mice were obtained from Vishva Dixit laboratory (Genentech, South San Francisco, CA, USA). $Myd88^{KO}$ and $TLR2^{KO}$ mice were obtained from Thierry Defrance (INSERM U851, France) and Nathalie Bonnefoy-Bérard (INSERM U851, France), respectively. $RIP3^{KO}$ and $RIP3Casp8^{DKO}$ femurs were obtained from Ed Mocarski (Emory Vaccine Centre, Atlanta, GA, USA). ASC^{KO}, $Casp1^{KO}$, $IFNAR1^{KO}$, $Myd88^{KO}$ and $TLR2^{KO}$ mice were bred at the PBES animal facility. For infection, mice were injected intradermally with 5×10^3 CFU of *F. novicida* strain U112 in 50 μl PBS. The mice were monitored for signs of sickness and lethality twice daily for the survival study. Alternatively, mice were euthanized at 48 h PI. Spleen and liver were harvested at 48 h PI, homogenised and dilutions were plated on supplemented Mueller Hinton plates. The bacterial burden in the spleen and the liver was determined to be similar in ASC^{KO} and $Casp1^{KO}$ mice. Blood was collected by intracardiac puncture. Following a 20-min incubation at 4° C, clotted blood was centrifuged at 15 000 r.p.m. during 15 min to obtain serum. IFN-γ levels in serum were determined by multiplex immunoassay (Bio Plex Pro Mouse Cytokines-Biorad, Marnes-la-Coquette, France) at the PBES genotyping and phenotyping platform.

Bone marrow-derived macrophages, dendritic cells, cell culture and transduction. Preparation, culture and infection of bone-marrow macrophages were performed as previously described.[13] To obtain BMDC, red blood cells were lysed using a hypotonic buffer and bone-marrow progenitors were cultured for 5 days in RPMI1640 medium (Invitrogen, Marnes-la-Coquette, France) supplemented with 5% FCS (Lonza, Basel, Switzerland), 50 μM β-mercapto-ethanol (Sigma, Saint-Quentin Fallavier, France), 2% v/v GM-CSF-containing J558-GMCSF supernatant. Retroviral particles were generated in Phoenix-Eco packaging cells by transfection with a modified pMSCV2.2 plasmid expressing either ASC-mCherry or GFP-AIM2 chimeric proteins (primers and cloning details are provided in Supplemental Information). Retroviral transduction was performed twice on fresh myeloid progenitors at day 2 and 3 post isolation from the bone marrow. Lentivirus particles were generated for the expression of Bcl-2, Bcl-X_L, FLAG tag peptide or FLAG-tagged prodomains of caspases-1, -8 and -9. Transduction of BMM was optimised in order to obtain transgene expression in more than 90% of cells, as assessed by flow cytometry analysis. Detailed protocols on lentivirus production and transduction, and description of the plasmids used can be found in the Supplemental Material and Methods. Transduced macrophages were infected 96 to 120 h post-transduction. When transduction or flow cytometry assays were performed, macrophages were plated on non-treated plastic plates to ease macrophage collection. 293T and Phoenix-Eco cells were cultured in DMEM medium, supplemented with 10% FBS, penicillin (100 U/ml), streptomycin (100 U/ml), 1 mM glutamine and 1 mM sodium pyruvate.

Bacterial strains, growth conditions and intracellular replication assay. *F. tularensis* subspecies *novicida* strain Utah (U112) and mutant lacking the whole FPI were grown in tryptic soy broth supplemented with 0.1% (w/v) cysteine. *F. novicida* U112 or ΔFPI mutant were chemically transformed with pKK-214-GFP to obtain GFP-expressing strains. Strains, plasmids and protocol details are provided in Supplemental Information.

For replication experiments, 3×10^5 macrophages were seeded per well in 2 cm^2 well. Macrophages were lysed at various times PI with 1% (w/v) saponin (Sigma) in water for 5 min, diluted and plated on TSA supplemented with 0.1% (w/v) cysteine to enumerate colony-forming units. Analysis of intracellular bacterial growth was also performed on a CantoII FACS (BD Biosciences, Le Pont de Claix, France) by detecting the fluorescence emission of intracellular GFP-expressing bacteria.

Cell death assays. Quantification of cell death was performed by analysis of LDH release in the cell supernatant, using the CytoTox96 LDH kit (Promega, Charbonnières-les-Bains, France), following manufacturer's instructions. A total of 10^5 BMM in a 0.3-cm^2 well in 120 μl of phenol-red^{minus} medium were used. Detection of phosphatidylserine in the outer layer of the plasma membrane was performed by Annexin V staining, using the Annexin V/FITC or Annexin V/APC assay kits (AbD Serotec, Düsseldorf, Germany), following manufacturer's instructions. Cell death was also quantified by monitoring propidium iodide incorporation. Briefly, 5×10^4 BMM were seeded in 0.3 cm^2 wells of black 96-flat-bottom-well plate, in phenol-red^{minus} medium. One hour after infecting cells with *F. novicida*, propidium iodide was added to each well at a final concentration of 5 μg/ml. Propidium iodide fluorescence was measured over a 24-h period on a microplate fluorimeter (Tecan, Lyon, France). Fluorescence in each well was normalised to the fluorescence obtained at 2 h PI. For the analysis of cell permeabilisation and nuclear condensation, 2.5×10^5 BMM were seeded onto glass coverslips in 24-well plate. At desired time following infection with *F. novicida*, cells were incubated with EtDi at 1 μM final concentration for 15 min at 37 °C. Cells were fixed by incubation with 4% (w/v) paraformaldehyde solution for 10 min, before performing three washes with PBS and staining with DAPI (100 ng/ml). Cells with condensed nuclei (small nuclei, no evident nucleolus) and intact cell membrane (no EtDi staining) were counted out of 200 cells in each coverslip. Nucleus size was measured using Image J software (NIH, Bethesda, MD, USA). Three replicates were prepared for each sample at each time point. Cells were imaged with a $\times 63$ objective with a Zeiss LSM 510 (Axiovert 100M, Jena, Germany). Nuclei of cells with fragmented DNA were stained with TUNEL, following manufacturer's instructions (in situ cell death fluorescein-Roche, Boulogne-Billancourt, France). A total of 10^5 BMM were seeded onto glass coverslips in 24-well plate. At desired time following infection, cells were fixed by incubation with 4% (w/v) paraformaldehyde solution for 10 min, then stained with TUNEL and DAPI. Cells were imaged with an inverted Zeiss (Le Pecq, France) 100M microscope and a $\times 63$ objective. The proportion of cells with fragmented DNA was obtained by counting $TUNEL^+$ cells out of a 200-cell population in each coverslip. Three replicates were prepared for each sample at each time point. For the assessment of DNA fragmentation by gel electrophoresis, 10^6 BMM were seeded in 6-well plate. Eight hours after infecting cells with U112 (MOI 100), or following a 4-h treatment with 5 μM gliotoxin, isolation of fragmented DNA was performed. Protocol is detailed in the Supplemental Material and Methods.

BMM transfection with p(dA/dT). Cell transfection was performed by using lipofectamine 2000 (Invitrogen) and following manufacturer' instructions. A total of 0.2 μg of poly(dA-dT)•poly(dT-dA) (p(dA/dT)) (Invivogen) and 0.5 μl of lipofectamine were used to transfect 5×10^4 BMM in a 0.3 cm^2 well.

Microarray analysis. Mouse exonic evidence based oligonucleotide arrays consisting of 70 nucleotide-long probes were used. Detailed protocols are available in Supplemental Material. Two biological replicates were realized for each sample at each time points.

Time-lapse analysis. A total of 7×10^5 cells were seeded onto a glass coverslip in 6-well plates. Following cell infection with *F. novicida* or p(dA/dT) transfection, the coverslip was transferred into a POC chamber system (Pecon, Erbach, Germany) and placed on a thermostated stage. Cells were imaged every 3 min for up to 4 h with an inverted Zeiss 100M microscope and a $\times 63$ objective. Image acquisition and analysis were performed by using the Image J and Metamorph (Molecular Devices, Sunnyvale, CA, USA) softwares.

Protein lysates and caspase activity assay. Following BMM infection, protein extracts were obtained by incubating cells with lysis buffer (10 mM Hepes/KOH, 2mM EDTA, 0.1% CHAPS, 250 mM sucrose, 5 mM dithiothreitol). Samples were clarified by centrifugation at 4 °C, 13 000 *g* for 15 min. Protein concentration was determined using Bradford method (BioRad). Fluorimetric analysis of caspase-3/7 activity was performed by incubating protein extracts (4 μg/sample) with Ac-DEVD-AMC at 40 μM final concentration. Fluorescent reading over 90 min was performed on a fluorimeter (Tecan).

Immunoblotting analysis. Protein lysates for immunoblotting were prepared by using the lysis buffer previously described, enriched with Complete protease inhibitor cocktail (Roche). Equal amounts of protein lysates (30 μg per sample for caspases-2, and -3; 10 μg/sample for caspase-8 and -9; 15 μg per sample for IκBα) were loaded in 4–12% Bis/Tris gel (Invitrogen), and run in MES buffer (caspase-2, -3, -9 and IκBα) or MOPS buffer (caspase-8) (Invitrogen). Protein transfer was performed with iBlot gel transfer stacks (Invitrogen). Antibodies anti–caspase–2 (kindly provided by Dr. J Yuan, 10^3 dilution), anti caspase-3 (sc-136219, Santa Cruz Biotechnology, Inc., Heidelberg, Germany, 10^3 dilution), anti caspase-8 (ALX-804-447, Enzo Life Sciences, Villeurbanne, France, 3×10^3 dilution), anti

caspase-9 (M054, MBL, Woburn, MA, USA, 10^4 dilution), anti IkB-α (9242, Cell Signaling, Beverly, MA, USA, 10^3 dilution) were used.

Co-immunoprecipitation. Protein extracts were obtained from 10^7 cells incubated for 20 min on ice with the following lysis buffer: 20 mM Tris HCl, pH 8.0; 150 mM NaCl; 1 mM EDTA, 10% glycerol; 1% NP-40; Complete protease inhibitor cocktail (Roche). Unbroken cells and nuclei were eliminated by centrifugation (2000 *g*, 15 min, 4 °C). Samples were then precleared with protein A-sepharose beads (Sigma), then incubated overnight at 4 °C with Rat-anti ASC antibody (kindly provided by S Mariathasan, Genentech), previously crosslinked with protein A-sepharose beads by using DSS (Thermo Scientific, Saint Herblain, France) and following manufacturer's instructions. Beads were washed five times, resuspended in loading buffer and heated at 95 °C for 5 min. Immunoblotting analysis for ASC and Caspase-8 were performed as described previously, using antibodies against ASC (sc-22515R, Santa Cruz) and caspase-8 (ALX-804-447, Enzo Life Sciences). The specificity of caspase-8 immunoblot was checked by using RIP3/Casp8^{DKO} macrophages.

Caspase inhibitors treatment. Caspase inhibitors (Z-DEVD-FMK, Ac-LEHD-CMK, Z-IETD-FMK, Z-VDVAD-FMK) purchased from Bachem (Bubendorf, Switzerland), were dissolved in DMSO, and added to cells 1 h post-*F. novicida* infection (DMSO not exceeding the 0.2% (v/v) of culture medium). Untreated cells were incubated in medium containing DMSO 0.2% (v/v).

Reconstitution of the inflammasome pathway in 293T cells. Sewing PCR for caspases prodomain/active caspase-1 domain, were performed by using primers listed in Supplemental Table S1. PCR products were cloned into a pEGFP-N1 vector (primers and cloning strategies are detailed in Supplemental Information). 4×10^4 293T cells were seeded in 0.3 cm^2 wells. Cells were transfected with 50 ng/well of plasmid expressing pro-IL-1β (p162.1), 25 ng/well of plasmid expressing either of the chimeric caspase proteins, 5 ng/well of plasmid expressing AIM2 (p200 plasmid) in presence or absence of 20 ng/well of plasmid for the expression of ASC (p115.1). Supernatants were collected 18 h post transfection and IL-1β levels were determined by ELISA (DuoSet, R&D systems, Lille, France).

Caspase colocalization assay. In all, 1.5×10^5 BMM were seeded onto glass coverslips in 24-well plate. Macrophages were incubated with FITC-labelled caspase-8 inhibitor IETD or caspase-9 inhibitor LEHD (ImmunoChemistry Technologies, Bloomington, MN, USA) 2 h after *F. Novicida* infection. Alternatively, macrophages expressing FLAG-tagged prodomains of caspase-1, -8 or -9 were obtained by lentiviral transduction. Cells were fixed with 4% (w/v) paraformaldehyde solution 8 h PI. Speck formation was assessed by antibody staining of endogenous AIM2 (Rat-anti-Aim2 antibody, Genentech) or ASC proteins (SC22514-R antibody, Santa Cruz). FLAG tag fusion proteins were detected thanks to the F3165 antibody (Sigma). Images were acquired thanks to an inverted confocal Zeiss LSM 510 microscope and a $\times 63$ objective.

AIM2 speck formation kinetics. Quantification of AIM2 speck formation was performed on GFP-AIM2-transduced primary macrophages. Three biological replicates for each investigated conditions were made and for each coverslip more than 200 cells were counted.

Statistical analysis. The statistical significances for *in vitro* data were determined by an unpaired t test analysis. Two-tailed *P* values are shown as follows: $^*P<0.05$; $^{**}P<0.01$. *In vivo* data were analysed by Mann–Whitney analysis; two-tailed *P* values are shown. $^{***}P<0.0001$.

Conflict of Interest

The authors declare no conflict of interest.

Acknowledgements. We thank V Dixit, E Mocarsky, J Upton and W Kaiser; L Genestier and T Defrance; N Bonnefoy-Bérard for ASC^{KO}, RIP3Casp8^{DKO}, Myd88^{KO} and TLR2^{KO} mice, respectively. We thank D Monack, P Broz and K Belhocine for AIM2^{KO} macrophages, B Py, J Yuan, S Mariathasan, and U Hasan for antibodies, R Tsien, S Yamada, S Méresse for plasmids. We thank R Vance and G Nolan for providing plasmids, cell lines and advice for retroviral transduction of primary macrophages, MC Michallet and S Djebali for purification of B and T cells, S Salcedo for protocols and advice on BMDC and Y Jamilloux for critical reading of the manuscript. We acknowledge the contribution of the PBES (P Contard, D Gallouche and S Blanc), PLATIM (C Chamot, C Lionnet), Cellulothèque (I Grosjean), flow cytometry (T Andrieu) platforms of SFR Biosciences Gerland-Lyon Sud (UMS344/US8). This work was supported by a Marie Curie reintegration grant (no.PIRG07-GA-2010-268399) and by a FINOVI Young investigator grant (http://www.finovi.org/en:start).

1. Bielecki J, Youngman P, Connelly P, Portnoy DA. Bacillus subtilis expressing a haemolysin gene from Listeria monocytogenes can grow in mammalian cells. *Nature* 1990; **345**: 175–176.
2. Martinon F, Burns K, Tschopp J. The inflammasome: a molecular platform triggering activation of inflammatory caspases and processing of proIL-beta. *Mol Cell* 2002; **10**: 417–426.
3. Brodsky IE, Monack D. NLR-mediated control of inflammasome assembly in the host response against bacterial pathogens. *Semin Immunol* 2009; **21**: 199–207.
4. Fernandes-Alnemri T, Wu J, Yu JW, Datta P, Miller B, Jankowski W *et al.* The pyroptosome: a supramolecular assembly of ASC dimers mediating inflammatory cell death via caspase-1 activation. *Cell Death Differ* 2007; **14**: 1590–1604.
5. Bergsbaken T, Fink SL, Cookson BT. Pyroptosis: host cell death and inflammation. *Nat Rev Microbiol* 2009; **7**: 99–109.
6. Miao EA, Leaf IA, Treuting PM, Mao DP, Dors M, Sarkar A *et al.* Caspase-1-induced pyroptosis is an innate immune effector mechanism against intracellular bacteria. *Nat Immunol* 2010; **11**: 1136–1142.
7. Keim PS, Johansson A, Wagner DM. Molecular Epidemiology, Evolution, and Ecology of Francisella. *Ann NY Acad Sci* 2007; **1105**: 30–66.
8. Hall JD, Woolard MD, Gunn BM, Craven RR, Taft-Benz S, Frelinger JA *et al.* Infected-host-cell repertoire and cellular response in the lung following inhalation of Francisella tularensis Schu S4, LVS, or U112. *Infect Immun* 2008; **76**: 5843–5852.
9. Golovliov I, Baranov V, Krocova Z, Kovarova H, Sjostedt A. An attenuated strain of the facultative intracellular bacterium Francisella tularensis can escape the phagosome of monocytic cells. *Infect Immun* 2003; **71**: 5940–5950.
10. Clemens DL, Lee BY, Horwitz MA. Virulent and avirulent strains of Francisella tularensis prevent acidification and maturation of their phagosomes and escape into the cytoplasm in human macrophages. *Infect Immun* 2004; **72**: 3204–3217.
11. Lindgren H, Golovliov I, Baranov V, Ernst RK, Telepnev M, Sjostedt A. Factors affecting the escape of Francisella tularensis from the phagolysosome. *J Med Microbiol* 2004; **53**: 953–958.
12. Mariathasan S, Weiss DS, Dixit VM, Monack DM. Innate immunity against Francisella tularensis is dependent on the ASC/caspase-1 axis. *J Exp Med* 2005; **202**: 1043–1049.
13. Henry T, Brotcke A, Weiss DS, Thompson LJ, Monack DM. Type I interferon signaling is required for activation of the inflammasome during Francisella infection. *J Exp Med* 2007; **204**: 987–994.
14. Jones JW, Kayagaki N, Broz P, Henry T, Newton K, O'Rourke K *et al.* Absent in melanoma 2 is required for innate immune recognition of Francisella tularensis. *Proc Natl Acad Sci USA* 2010; **107**: 9771–9776.
15. Fernandes-Alnemri T, Yu JW, Juliana C, Solorzano L, Kang S, Wu J *et al.* The AIM2 inflammasome is critical for innate immunity to Francisella tularensis. *Nat Immunol* 2010; **11**: 385–393.
16. Rathinam VA, Jiang Z, Waggoner SN, Sharma S, Cole LE, Waggoner L *et al.* The AIM2 inflammasome is essential for host defense against cytosolic bacteria and DNA viruses. *Nat Immunol* 2010; **11**: 395–402.
17. Fernandes-Alnemri T, Yu JW, Datta P, Wu J, Alnemri ES. AIM2 activates the inflammasome and cell death in response to cytoplasmic DNA. *Nature* 2009; **458**: 509–513.
18. Hornung V, Ablasser A, Charrel-Dennis M, Bauernfeind F, Horvath G, Caffrey DR *et al.* AIM2 recognizes cytosolic dsDNA and forms a caspase-1-activating inflammasome with ASC. *Nature* 2009; **458**: 514–518.
19. Mariathasan S, Weiss DS, Newton K, McBride J, O'Rourke K, Roose-Girma M *et al.* Cryopyrin activates the inflammasome in response to toxins and ATP. *Nature* 2006; **440**: 228–232.
20. Henry T, Monack DM. Activation of the inflammasome upon Francisella tularensis infection: interplay of innate immune pathways and virulence factors. *Cell Microbiol* 2007; **9**: 2543–2551.
21. Kang SJ, Wang S, Hara H, Peterson EP, Namura S, Amin-Hanjani S *et al.* Dual role of caspase-11 in mediating activation of caspase-1 and caspase-3 under pathological conditions. *J Cell Biol* 2000; **149**: 613–622.
22. Kayagaki N, Warming S, Lamkanfi M, Vande Walle L, Louie S, Dong J *et al.* Non-canonical inflammasome activation targets caspase-11. *Nature* 2011; **479**: 117–121.
23. Kalai M, Lamkanfi M, Denecker G, Boogmans M, Lippens S, Meeus A *et al.* Regulation of the expression and processing of caspase-12. *J Cell Biol* 2003; **162**: 457–467.
24. Jesenberger V, Procyk KJ, Yuan J, Reipert S, Baccarini M. Salmonella-induced caspase-2 activation in macrophages: a novel mechanism in pathogen-mediated apoptosis. *J Exp Med* 2000; **192**: 1035–1046.
25. Burckstummer T, Baumann C, Bluml S, Dixit E, Durnberger G, Jahn H *et al.* An orthogonal proteomic-genomic screen identifies AIM2 as a cytoplasmic DNA sensor for the inflammasome. *Nat Immunol* 2009; **10**: 266–272.

26. Roberts TL, Idris A, Dunn JA, Kelly GM, Burnton CM, Hodgson S *et al.* HIN-200 proteins regulate caspase activation in response to foreign cytoplasmic DNA. *Science* 2009; **323**: 1057–1060.
27. Hasegawa M, Kawase K, Inohara N, Imamura R, Yeh WC, Kinoshita T *et al.* Mechanism of ASC-mediated apoptosis: bid-dependent apoptosis in type II cells. *Oncogene* 2007; **26**: 1748–1756.
28. Hasegawa M, Imamura R, Kinoshita T, Matsumoto N, Masumoto J, Inohara N *et al.* ASC-mediated NF-kappaB activation leading to interleukin-8 production requires caspase-8 and is inhibited by CLARP. *J Biol Chem* 2005; **280**: 15122–15130.
29. Masumoto J, Dowds TA, Schaner P, Chen FF, Ogura Y, Li M *et al.* ASC is an activating adaptor for NF-kappa B and caspase-8-dependent apoptosis. *Biochem Biophys Res Commun* 2003; **303**: 69–73.
30. McConnell BB, Vertino PM. Activation of a caspase-9-mediated apoptotic pathway by subcellular redistribution of the novel caspase recruitment domain protein TMS1. *Cancer Res* 2000; **60**: 6243–6247.
31. Ohtsuka T, Ryu H, Minamishima YA, Macip S, Sagara J, Nakayama KI *et al.* ASC is a Bax adaptor and regulates the p53-Bax mitochondrial apoptosis pathway. *Nat Cell Biol* 2004; **6**: 121–128.
32. Kantari C, Walczak H. Caspase-8 and bid: caught in the act between death receptors and mitochondria. *Biochem Biophys Acta* 2011; **1813**: 558–563.
33. Aliprantis AO, Yang RB, Weiss DS, Godowski P, Zychlinsky A. The apoptotic signaling pathway activated by Toll-like receptor-2. *EMBO J* 2000; **19**: 3325–3336.
34. Van Herreweghe F, Festjens N, Declercq W, Vandenabeele P. Tumor necrosis factor-mediated cell death: to break or to burst, that's the question. *Cell Mol Life Sci* 2010; **67**: 1567–1579.
35. Kaiser WJ, Upton JW, Long AB, Livingston-Rosanoff D, Daley-Bauer LP, Hakem R *et al.* RIP3 mediates the embryonic lethality of caspase-8-deficient mice. *Nature* 2011; **471**: 368–372.
36. Gurcel L, Abrami L, Girardin S, Tschopp J, van der Goot FG. Caspase-1 activation of lipid metabolic pathways in response to bacterial pore-forming toxins promotes cell survival. *Cell* 2006; **126**: 1135–1145.
37. Motani K, Kushiyama H, Imamura R, Kinoshita T, Nishiuchi T, Suda T. Caspase-1 protein induces apoptosis-associated speck-like protein containing a caspase recruitment domain (ASC)-mediated necrosis independently of its catalytic activity. *J Biol Chem* 2011; **286**: 33963–33972.
38. Hasegawa M, Imamura R, Motani K, Nishiuchi T, Matsumoto N, Kinoshita T *et al.* Mechanism and repertoire of ASC-mediated gene expression. *J Immunol* 2009; **182**: 7655–7662.
39. Gringhuis SI, Kaptein TM, Wevers BA, Theelen B, van der Vlist M, Boekhout T *et al.* Dectin-1 is an extracellular pathogen sensor for the induction and processing of IL-1beta via a noncanonical caspase-8 inflammasome. *Nat Immunol* 2012; **13**: 246–254.
40. Bruey JM, Bruey-Sedano N, Luciano F, Zhai D, Balpai R, Xu C *et al.* Bcl-2 and Bcl-XL regulate proinflammatory caspase-1 activation by interaction with NALP1. *Cell* 2007; **129**: 45–56.

Supplementary Information accompanies the paper on Cell Death and Differentiation website (http://www.nature.com/cdd)